AIAA 81-2477R

Comparison of Shuttle Flight Pressure Data to Computational and Wind-Tunnel Results

P.F. Bradley,* P.M. Siemers III,* and K. James Weilmuenster*
NASA Langley Research Center, Hampton, Va.

A comparison between orbiter development flight instrumentation (DFI) forward fuselage flight pressure data, obtained from OV-102 during the space transportation system's (STS-1) re-entry, and ground facility and computational results is presented. Wind-tunnel data were obtained on a 0.04-scale orbiter forebody model. Computational data were obtained from the high alpha inviscid solutions (HALIS) computer code. These comparisons will be used to validate the existing experimental data base and optimize pressure modeling techniques developed in support of the Shuttle entry air data system (SEADS). The SEADS is a proposed across-the-speed-range second-generation air data system for the orbiter, using an array of flush pressure taps to be installed in the orbiter nose cap and forward fuselage. Knowledge derived from these comparisons will contribute to an improved capability to predict the performance of existing flight systems as well as an improved capability to design space transportation and general flight systems.

Nomenclature

M_∞ = freestream Mach number
P = pressure, Pa
Q = dynamic pressure, Pa
X, Y, Z = model coordinates, m
α = angle of attack, deg
β = angle of sideslip, deg

Introduction

THE space transportation system (STS)—the-state-of-the-art in space transportation systems—although a result of a rigorous, ground-based design, development, and test program did not undergo a traditional total system prototype flight test program. The STS test program is unique in that it combines flight testing with operational flights using the first operational orbiter vehicle (OV-102).

To verify the re-entry performance of the Space Shuttle Orbiter and thus verify the preflight design, development, and test programs, the orbiter has been instrumented to obtain various types of flight data. This instrumentation, designated development flight instrumentation (DFI), includes pressure transducers, thermocouples, calorimeters, and accelerometers placed at approximately 3400 locations on/in the vehicle. In addition to the basic orbiter performance verification requirements, the Office of Aeronautics and Space Technology's (OAST) orbiter experiment program (OEX) has established a need "to utilize the Space Shuttle capabilities to obtain research and technology data with which to advance aerospace technology."[2] This program, through extensive research, has defined a need for more extensive and specific instrumentation to complete the flight research base. The Shuttle entry air data system (SEADS), along with other OEX instrumentation systems, and the DFI will support flight research being conducted by NASA relative to aerodynamics and aerothermodynamics.

In support of the development of the SEADS, a 0.04-scale model of the orbiter's forebody was tested in various wind-tunnel facilities. The SEADS model was instrumented to model much of the forward fuselage DFI, providing an opportunity to verify both experimental and analytical forebody pressure predictions. A high confidence in the orbiter pressure model generated from data obtained in ground-based facilities is essential to confidence in the results of other analyses related to flowfield phenomena involving pressure levels and distributions. Confidence in the pressure algorithm being used for data analysis is the key to success of the SEADS and its eventual use as an operational air data system.

Model and Instrumentation

The model used in the wind-tunnel tests is a 0.04-scale model of the orbiter's forebody. The model extends to that length which would be X station 11.43 m ($X_0 = 450$ in.) in the orbiter's coordinate system. The portion of the orbiter modeled is shown in Fig. 1. The DFI locations used in this comparison are shown in Figs. 1-3. The locations of the DFI on the orbiter were provided by the manufacturer and were used in the development of the 0.04-scale model. The model was fabricated from cast 17-4 stainless steel with thickness ranging from 0.00635 m at the most forward point to 0.0305 m near the center of the model where the reaction control system jets were modeled. A photograph of the model is shown in Fig. 4.

The model is instrumented with 72 flush orifices corresponding to SEADS and DFI pressure locations on the orbiter. The instrumentation also includes two chromel-alumel thermocouples which are located near the nose of the model on the back surface of the skin. These thermocouples were used only as indicators of model temperature for those wind tunnels in which model heating could limit run time. A list of model orifices used for comparison with flight data and their model coordinate locations is given in Table 1, while the model orifice number to orbiter DFI surface pressures number correspondence is listed in Table 2. The model coordinate system is shown in Fig. 5.

In order to provide a comprehensive data base for the development of the SEADS pressure model, the orbiter forebody model was tested in several wind tunnels. Although an extensive test matrix was accomplished in each facility, this paper discusses only those tunnel test conditions that closely match STS-1 flight data.

The model was tested in the continuous flow hypersonic tunnel (CFHT), the unitary plan wind tunnel, and the 20-in.

Presented as Paper 81-2477 at the AIAA/SETP/SFTE/SAE/ITEA/IEEE 1st Flight Testing Conference, Las Vegas, Nev., Nov. 11-13, 1981; submitted Nov. 16, 1981; revision received April 14, 1982.

*Aerospace Engineer, Aerothermodynamics Branch, Space Systems Division.

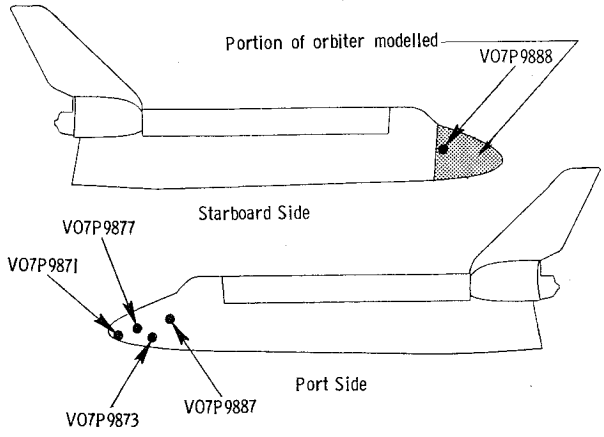

Fig. 1 DFI locations on port and starboard sides of orbiter.

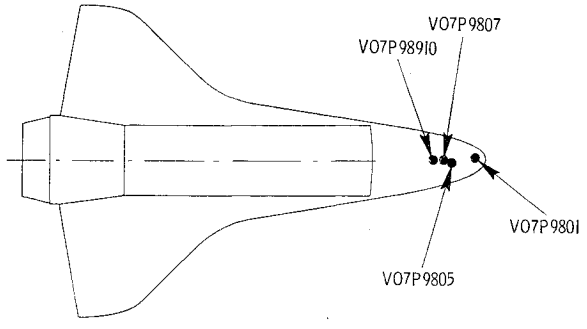

Fig. 2 DFI locations on upper surface of orbiter.

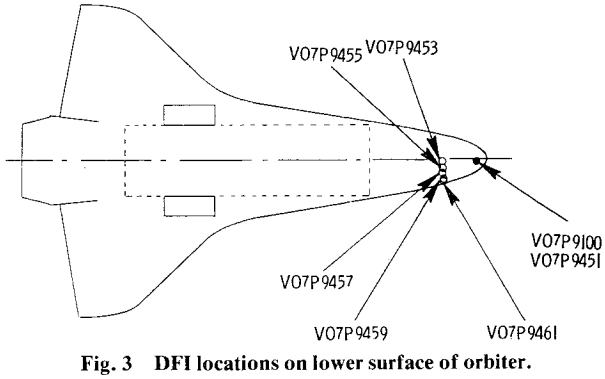

Fig. 3 DFI locations on lower surface of orbiter.

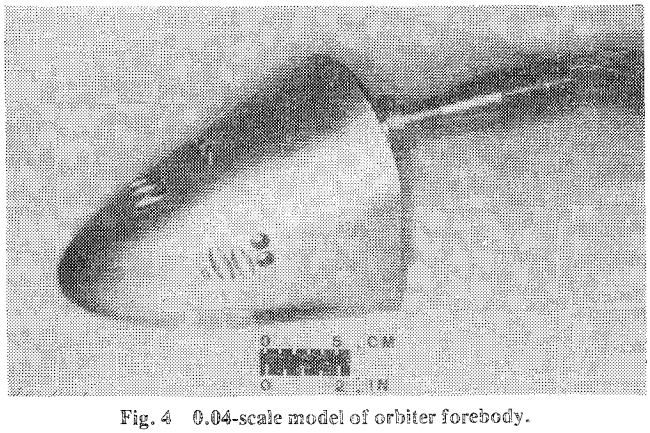

Fig. 4 0.04-scale model of orbiter forebody.

Mach-6 air tunnel. The CFHT, a Mach-10 air facility with a 0.787-m (31-in.) test section is described in Refs. 2 and 3. The angle-of-attack range (α) was from -5 to 45 deg and the angle-of-sideslip range (β) was from -3 to 3 deg. The tunnel's

Table 1 Model orifice locations

Model orifice	X, m	Y, m	Z, m
215	0.1957	−0.00307	−0.03774
216	0.1958	−0.03703	0.01150
218	0.1959	−0.00520	0.03297
225	0.1236	0.00012	−0.07321
235	0 1010	−0.07043	0.02940
236	0.1003	−0.06227	0.03984
237	0.0950	−0.04135	0.05060
238	0.09624	−0.02631	0.05331
239	0.09521	−0.00495	0.05498
244	0.0699	0.00101	−0.09529
245	0.1009	0.00105	−0.08257
246	0.1404	−0.0607	−0.00459
247	0.0950	−0.07519	0.01804
248	0.03820	−0.08739	−0.03331
249	0.03822	0.08758	0.03352

Table 2 Orbiter DFI locations

DFI locations	Corresponding model orifice
V07P9100	218
V07P9451	218
V07P9453	239
V07P9455	238
V07P9457	237
V07P9459	236
V07P9461	235
V07P9801	215
V07P9805	225
V07P9807	245
V07P9810	244
V07P9871	216
V07P9873	247
V07P9877	246
V07P9887	248
V07P9888	249

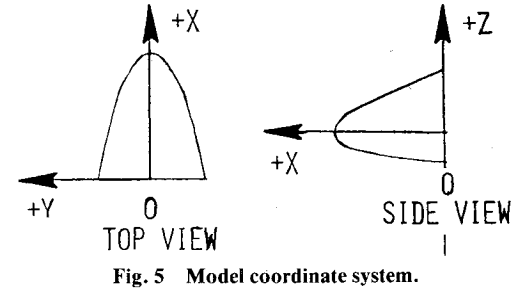

Fig. 5 Model coordinate system.

Wind-tunnel data at Mach 6 were obtained in the 20-in. Mach-6 air tunnel. This facility is of the blow-down type with a test core of 0.41-m square in the 0.508 by 0.508-m (20-in.) test section. It is described in Refs. 2 and 3. The angle-of-injection system is located on the side of the tunnel with model/sting assembly mounted on an injection plate which is flush with the tunnel's sidewall at full model injection. The core of uniform flow is approximately 0.355-m (14-in.) square at the Reynolds number tested. The size of the injection plate along with the core-of-uniform-flow size limits test conditions with this large model/sting assembly.

attack range was from 0 to 35 deg and the angle of sideslip from 0 to -4 deg.

For the Mach number range from 2.3 to 4.65, the model was tested in the high Mach number test section of the unitary plan wind tunnel. This variable pressure tunnel operates continuously with an asymmetrical sliding block nozzle which permits a continuous variation in the test-section Mach

number from 2.3 to 4.65. This facility is described in Ref. 4. The angle-of-attack range was from −2.5 to 30 deg and the angle of sideslip from −5 to +5 deg.

For the low supersonic speed range, wind-tunnel results were obtained in the low-speed test section of the unitary tunnel. The angle-of-attack and sideslip ranges were the same as in the high-speed leg.

Flight Data/Wind-Tunnel Comparisons

The comparison of STS-1 flight data with ground-based facility data includes the portion of the re-entry trajectory shown in Fig. 6. This figure shows the correlation between the flight profile data (solid line), the data obtained from the wind tunnel (open symbols), and the computational results (closed symbols). A corresponding list of flight Mach number, flight angle of attack, flight angle of sideslip, wind-tunnel Mach number, Greenwich mean time (GMT) in the trajectory, and vehicle altitude is given in Table 3.

Data comparisons for the DFI locations were limited by transducer saturation during re-entry. Only one of the DFI locations studied has a 0-15-psi transducer. The time of saturation for each transducer is shown in Fig. 7 on the altitude vs GMT time plot. Examples of comparisons between an orbiter DFI location and a corresponding location on the 0.04-scale model are shown in Figs. 8-11. Additionally, data obtained from the HALIS computer code are also plotted. The HALIS data will be discussed in the next section. The symbols on Figs. 8-11 correspond to wind-tunnel (open symbols) and HALIS (closed symbols) data at specific Mach numbers. The type of symbol corresponds to the same type of symbol in Fig. 6. Thus, the open circle corresponds to a wind-tunnel Mach number of 10, and so forth.

The flight data were nondimensionalized by navigation-derived freestream dynamic pressure. Wind-tunnel data were nondimensionalized by the tunnel's freestream dynamic pressure at the test conditions. Data comparisons are especially good for the lower Mach numbers from data obtained in the unitary plan wind tunnel (Mach number range from 4.63 to 1.5) and data obtained in the Mach-6 air tunnel. Data obtained in the CFHT compares fairly well, but some of the tunnel data points are far from the flight data. Data from the wind-tunnel model lower surface locations corresponding

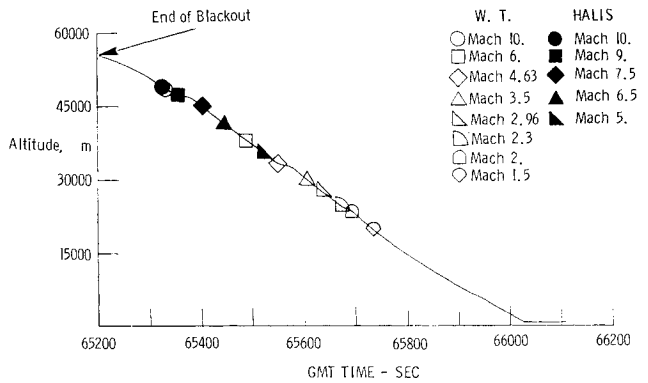

Fig. 6 Portion of reentry trajectory used for data comparisons.

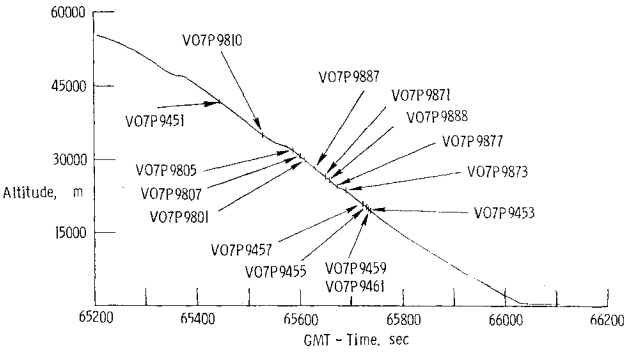

Fig. 7 Transducer saturation points in the trajectory.

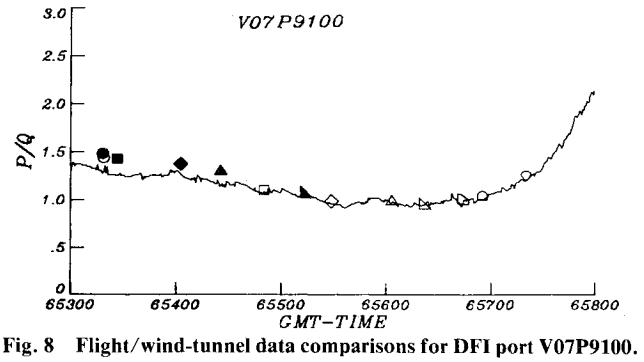

Fig. 8 Flight/wind-tunnel data comparisons for DFI port V07P9100.

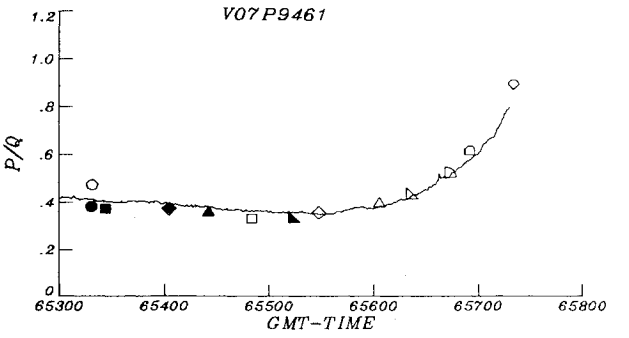

Fig. 9 Flight/wind-tunnel data comparisons for DFI port V07P9461.

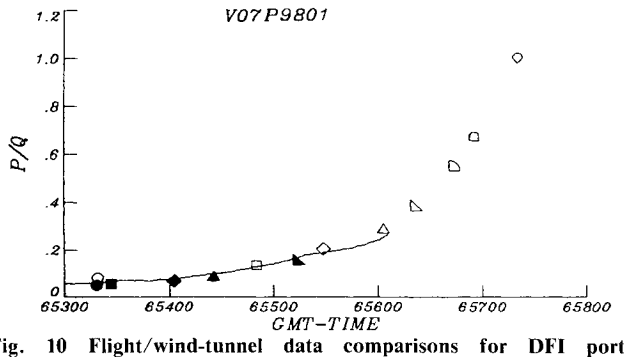

Fig. 10 Flight/wind-tunnel data comparisons for DFI port V07P9801.

Table 3 Flight conditions at wind-tunnel Mach numbers

Flight, M_∞	Flight, α	Flight, β	GMT (STS-1)	Altitude, km	Wind tunnel, M_∞
10.063	35.5	0.395	65332	49.17	10.02
6.0	25.0	−0.174	65484	38.91	6.0
4.625	20.0	−0.264	65548	33.87	4.63
3.5	18.0	0.4955	65606	30.48	3.5
2.9375	16.0	0.463	65636	27.87	2.95
2.3125	12.48	0.0248	65673	24.87	2.3
2.0	11.0	0.035	65692	23.72	2.0
1.5	9.25	1.44	65734	20.05	1.5

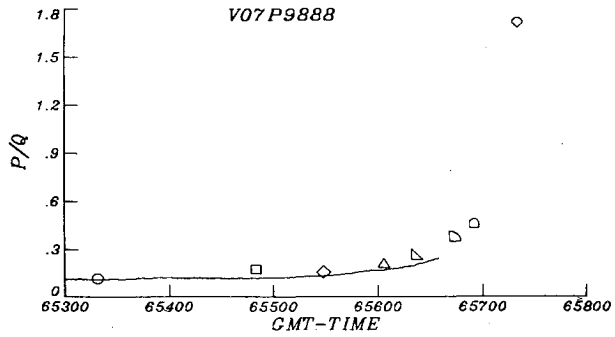

Fig. 11 Flight/wind-tunnel data comparisons for DFI port V07P9888.

to DFI measurements V07P9453, V07P9455, and V07P9457 at Mach 10 were far enough above the flight data and the other wind-tunnel points that their accuracy is suspect. Previous tests with large models in the CFHT have produced similar problems on the lower surfaces of such models at angles of attack of 35 deg and above. This problem is being attributed to the possibility that a reflected bow shock is interacting with the model's lower surface at high angle of attack. Since the orbiter's angle of attack at Mach 10 during STS-1 was greater than 35 deg, the accuracy of the wind-tunnel data for comparison to flight to Mach 10 requires additional research.

Comparison of Flight Data with Computation Results

Results obtained from the HALIS computer code are also plotted on the data in Figs. 8-11.[5] The HALIS data computed at flight Mach number and angle of attack are shown by the filled symbols. DFI locations on the forward fuselage of the orbiter were matched to the geometry used in the HALIS code and surface pressures at those locations were interpolated between mesh points in the computational geometry. The HALIS code, through a solution of the Euler equations, provides surface pressure information that agrees very well with wind-tunnel and flight data. Where accuracy on the lower surface Mach-10 wind-tunnel data is questioned, the HALIS data fill in with a good match to flight (Fig. 9). HALIS data also provide information between the wind-tunnel data available at Mach 10 and Mach 6 with good match to flight.

Since the flow on leeside of the orbiter is dominated by viscous phenomena, the HALIS solution could be invalid in the leeside flowfield. Therefore, the complex leeside geometry used for this study has been modified, as shown in Fig. 12, to simplify the computational problem and to allow a greater portion of the computer resources to be used for better resolution of the windward surface flowfield. HALIS data shown in Fig. 10 for V07P9801 agree very well with the flight data even though this port is located on the lee surface. This is due to the fact that this port is close to the nose, which is not dominated by viscous phenomena, and geometry simulation in this region is better than farther back on the vehicle. Figure 11 shows data obtained from V07P9888 located on the starboard side far back from the nose. HALIS data are not shown since the geometry differences between HALIS and the orbiter resulted in computer pressure distributions in this region that did not agree with flight and the wind-tunnel data. The use of the correct geometry in this region could provide better agreement.

The use of data from the HALIS code provides additional confidence in the interpretation of the wind-tunnel and flight data comparisons. HALIS data support the agreement observed between the wind-tunnel and flight data and lend confidence to predictions of forward fuselage pressure distributions with wind-tunnel data. The use of the wind-tunnel data for verification of orbiter performance and for the development of SEADS software is enhanced by the improved confidence when three sources of data agree as well as shown here.

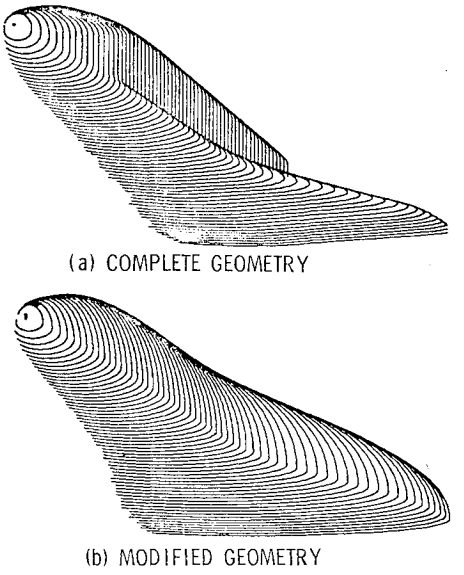

Fig. 12 Complete and modified orbiter geometry.

Concluding Remarks

A comparison between Space Shuttle Orbiter STS-1 pressure data and wind-tunnel pressure data has been made. Space Shuttle Orbiter DFI locations were matched to orifices on a 0.04-scale model of the orbiter's forward fuselage. Flight data were obtained at those trajectory points which matched the Mach numbers attainable in the wind tunnels. Flight data were nondimensionalized by navigation-derived freestream dynamic pressure and wind-tunnel data, by the tunnel's freestream dynamic pressure.

The best data comparisons were those obtained in the unitary plan wind tunnel, and the Mach-6 air tunnel for the low hypersonic to low supersonic range. Data comparisons for some DFI transducers were limited by transducer saturation during reentry.

A comparison was made between the flight and wind-tunnel data and computational data obtained from the HALIS code. The code determines the flowfield about the orbiter by solution of the Euler equations. To maximize the resolution of a majority of the windward flowfield, the lee surface geometry has been modified to reduce computer storage space for mesh points. Windward surface comparisons are excellent with both flight and wind-tunnel data. Comparisons with lee surface data close to the front of the orbiter are good, but as the computational geometry differs more from the actual orbiter geometry on the leeside, HALIS pressure data differ from flight and wind-tunnel data as expected. The good agreement among the three sources of data lends credibility to forward fuselage pressure distribution prediction techniques based on wind-tunnel data and thus the pressure model being developed for SEADS flight data analysis.

References

[1] Siemers, P.M. III and Larson, T.J., "Space Shuttle Orbiter and Aerodynamic Testing," *Journal of Spacecraft and Rockets*, Vol. 16, July-Aug. 1979, p. 223.

[2] Shafer, W.T. Jr., "Characteristics of Major Active Wind Tunnels at the Langley Research Center," NASA TMX-1130, July 1965.

[3] Pirrelo, C.T., Hardin, R.D., Heckart, M.V., and Brown, K.R., "An Inventory of Aeronautical Ground Research Facilities," Vol. I-Wind Tunnels, NASA CR-1874, Nov. 1971.

[4] "Manual for Users of the Unitary Plan Wind-Tunnel Facilities of the National Advisory Committee for Aeronautics NASA," 1956.

[5] Wielmuenster, K.J. and Hamilton, H.H. III, "A Method for Computation of Inviscid Three-Dimensional Flow Over Blunt Bodies Having Large Embedded Subsonic Regions," AIAA Paper 81-1203, June 1981.